Rapid Communications

Room temperature polar structure and multiferroicity in $BaFe_2Se_3$

W. Zheng,[1] V. Balédent,[1] M. B. Lepetit,[2,3] P. Retailleau,[4] E. V. Elslande,[4] C. R. Pasquier,[1] P. Auban-Senzier,[1] A. Forget,[5] D. Colson,[5] and P. Foury-Leylekian[1,*]

[1]*Laboratoire de Physique des Solides, CNRS, Univ. Paris-Sud, Université Paris-Saclay, 91405 Orsay Cedex, France*

[2]*Institut Néel, 38042 Grenoble, France*

[3]*Institut Laue Langevin, 38000 Grenoble, France*

[4]*Institut de Chimie des Substances Naturelles, CNRS UPR 2301, Université Paris-Sud, Université Paris-Saclay, 1 avenue de la Terrasse, 91198 Gif-sur-Yvette, France*

[5]*SPEC, CEA, CNRS-UMR3680, Université Paris-Saclay, Gif-sur-Yvette Cedex 91191, France*

(Received 10 May 2019; revised manuscript received 25 October 2019; published 6 January 2020)

The understanding of the superconducting phase under pressure in the famous iron-based spin ladder $BaFe_2Se_3$ commands a perfect understanding of the structural properties. We present an accurate single crystal x-ray analysis which demonstrates that the structure admitted until now at room temperature is totally ruled out. We show that the system has a polar structure already at 300 K and is thus ferroelectric. Its structure is modified below the Néel transition and the polarization is intensified. These features unambiguously prove the multiferroic character of $BaFe_2Se_3$ as proposed theoretically. This system evidences a competition between multiferroicity and superconductivity.

DOI: 10.1103/PhysRevB.101.020101

Most remarkable properties in solids such as superconductivity or multiferroicity arise from electronic correlations at a microscopic level. As a consequence of the quantum nature of their origin, such properties often appear at low temperature, drastically restricting their potential applications. Therefore, the discovery of new materials with nearby room temperature transitions are of particular interest. The iron chalcogenide $BaFe_2Se_3$ is one of them, with a magnetic ordering around 250 K [1] which is expected to couple with the lattice to create ferroelectricity [2]. This potential magnetoelectric multiferroic is further intriguing since it becomes a superconductor under pressure [3]. Since its structure is depicted by two iron ladders per unit cell, this system is one of the few one-dimensional iron superconductors. From an electronic point of view, this system is described as an orbital-selective Mott insulator [4] which may be responsible for the unconventional block magnetism observed by powder neutron diffraction experiment [5,6]. Thanks to these numerous remarkable properties, this system has recently been the subject of many experimental and theoretical studies. Its low dimensionality, conducive to more accurate calculations and simulations, leads to a considerable amount of theoretical investigations and predictions [2,5,7,8]. However, the starting point to understand this system is to have an accurate description of its atomic structure. The literature on this subject reports quite contradictory results. A powder neutron diffraction experiment shows a lattice distortion without symmetry loss evidence below T_N [9], indicating a strong magnetoelastic effect. Another study using powder neutron diffraction combined with neutron pair distribution function (PDF) suggests that the n glide plane may be lost across the magnetic transition at a local scale [1]. Two subsequent indistinguishable structures are proposed compatible with the average space group $Pmc2_1$. However, the lack of accurate atomic position and unambiguous space group determination above and below the Néel temperature prevents further precise theoretical studies and experimental works.

In this Rapid Communication, we present the results of our single crystal x-ray diffraction experiments to demonstrate the actual polar structure at room temperature of $BaFe_2Se_3$ and its evolution below the magnetic transition, unambiguously proving the multiferroic nature of this material below 200 K.

$BaFe_2Se_3$ single crystals were grown using a melt-growth method [10]. Starting mixtures for crystal growth were prepared using small pieces of Ba (99.9%), powder of Fe (99.9%), and of Se (99.999%). Two grams of reagents were weighed, mixed, and the resulting pellets, with the nominal composition 123, were placed in a carbon crucible and then sealed in an evacuated quartz tube and a partial pressure of 300 mbar of Ar gas. Typical growth conditions were as follows: the sample was heated at 1150 °C and melted for 24 h. The temperature was afterwards lowered to 750 °C at a rate of 5 °C/h, and the furnace was cooled down to room temperature at 100 °C/h. We obtained needlelike single crystals aggregated. The experimental details concerning the characterization of the samples are given in the Supplemental Material [11].

We performed x-ray diffraction measurements with a Rigaku XtaLabPro four-circle diffractometer at the ICSN laboratory using the Mo $K\alpha$ radiation emitted by a MM-003 microfocus sealed tube and equipped by a Dectris PILATUS3R-200K-A detector. The measurements were performed at room temperature and 150 K for two small single crystals ($S1$ and $S2$ of about $200 \times 30 \times 30\ \mu m^3$) from different batches. The crystallographic quality of the samples is attested by the

*Corresponding author: pascale.foury@u-psud.fr

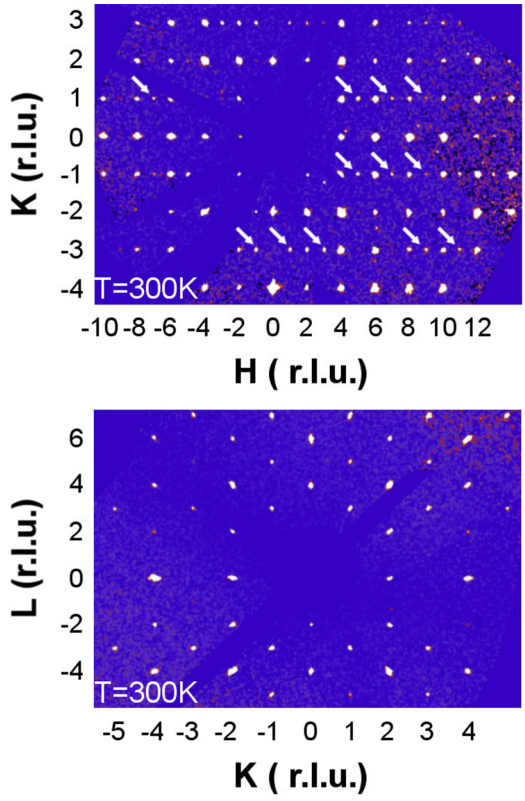

FIG. 1. Reconstructions of the lattice node planes $(H, K, 0)$ (up) and $(0, K, L)$ (down) of $BaFe_2Se_3$ (sample $S1$) at 300 K, taking into account absorption correction. Arrows indicate the forbidden reflections associated with the **a** glide planes.

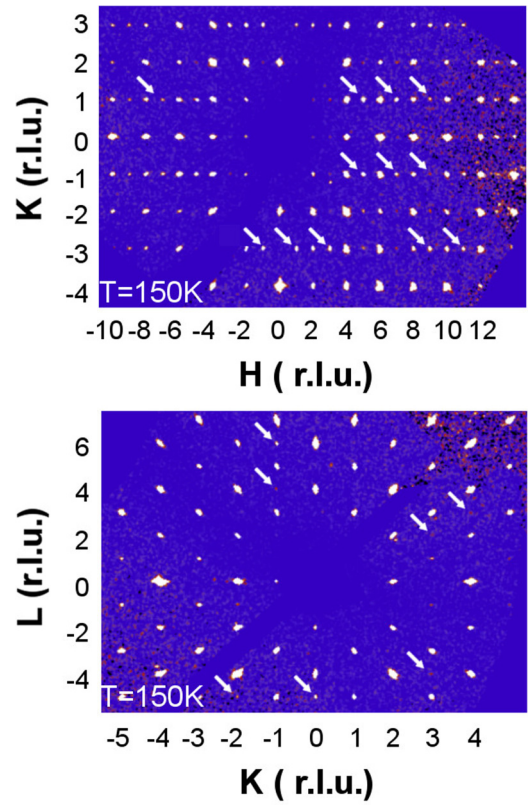

FIG. 2. Reconstructions of the lattice node planes $(H, K, 0)$ (up) and $(0, K, L)$ (down) of $BaFe_2Se_3$ (sample $S1$) at 150 K, taking into account absorption correction. Arrows in the down panel indicate the forbidden reflections associated with the **n** glide planes.

perfectly isolated Bragg reflections observed in the reciprocal reconstructions of Figs. 1 and 2. The magnetic properties of the two compounds were characterized with the commercial superconducting quantum interference device magnetometer (Quantum Design) of the LPS laboratory. From susceptibility measurements and neutron diffraction experiments (see Supplemental Material [11]), we have determined a T_N of 210 ± 10 K and 185 ± 10 K for the samples $S1$ and $S2$, respectively. These temperatures of magnetic ordering are consistent with previous works showing a T_N which spreads around 200 K [12,13] and even in a larger domain from 140 to 256 K [1,9,10,14]. This large range of T_N is expected to be due to slight deviations from the ideal $BaFe_2Se_3$ stoichiometry [15]. For the two samples measured in this work, the deviation from the perfect Fe stoichiometry have been checked by field emission scanning electron microscopy coupled with energy dispersive x-ray spectroscopy and does not exceed 2% (see Supplemental Material [11]). It is important to notice that all the physical properties of our compounds are similar to those published in various papers [1,9,10,12–14]. We have indeed the same powder x-ray diffractograms and the magnetic order stabilized below T_N presents the same propagation wave vector and the same block-like structure as in the references above. So we are confident that the deviation from the exact Fe stoichiometry at the origin of the decrease of T_N in our samples does not affect the structure and in particular its symmetry.

In the *Pnma* space group in which $BaFe_2Se_3$ crystallizes, the **a** glide plane induces that the $HK0$ Bragg reflections are forbidden whenever H are odd while the **n** glide plane implies that the $0KL$ reflections are forbidden when $K + L$ is odd. Figure 1 displays reciprocal lattice reconstructions of the $0KL$ and $HK0$ planes for $BaFe_2Se_3$ at 300 K. One can first observe that the reflections forbidden by the **n** glide plane are absent as expected. But interestingly, for the two compounds studied, the forbidden reflections associated with the **a** glide plane were systematically observed. More than 40 forbidden reflections with $I > 3\sigma$ were detected. The width of the forbidden reflections' profiles being comparable to that of the allowed Bragg reflections, one can exclude a disorder origin for these reflections. In addition their average intensity was about 4% of the average intensity of the standard Bragg reflections. This corresponds to a strong symmetry breaking of the **a** plane. Furthermore, the forbidden reflections are observed not only at low diffraction angles but also at high angles which suggests a displacive origin. In that case, the intensity of the forbidden reflections is expected to be proportional to the square of the atomic displacements which here gives 0.2 Å. These displacements are strongly larger than the ones generally observed for structural transitions like the Peierls transitions in the blue bronze [16] or in the spin Peierls $CuGeO_3$ system [17].

Before going any further, we checked for possible experimental artifacts. We verified that neither a wavelength

harmonic contamination ($\lambda/2$) nor the twinning of the crystal could explain the presence of such forbidden reflections. The possibility of multiple scattering effect was also ruled out since it could not affect only the reflections forbidden by the **a** glide plane. The observed forbidden reflections thus cannot be associated with an experimental artifact, and since they are observed in two compounds from different batches, we can conclude that this superstructure is an intrinsic structural property of $BaFe_2Se_3$ at 300 K. It was not evidenced in previous structural works because these experiments were performed on powders. In our more accurate work, we used single crystal x-ray measurements which enable us to detect very weak structural effects associated with the symmetry breaking observed.

At 150 K, below the magnetic ordering, the structures have been measured and the reciprocal lattice reconstructions of the $0KL$ and $HK0$ planes are given in Fig. 2. Forbidden reflections of the **a** glide plane are still present on the reconstructions and with the same average intensity. But 15 additional reflections forbidden by the **n** glide plane have appeared. Their intensity is about 1% of the average intensity of the standard Bragg reflections, they have the experimental resolution and behave as a displacive effect.

We will first discuss the data at 300 K. In light of our results, one can unambiguously assert that at 300 K, the space group cannot be *Pnma*. Among the orthorhombic space groups, compatible with all the experimentally observed reflections, two are proposed by the Jana software [18]. Firstly one finds $Pnm2_1$ ($Pmn2_1$ in the conventionnal setting) which is the subgroup of *Pnma* including the symmetry breaking of the **a** glide plane. The second possible space group is *Pnmm* (*Pmmn* in the standard setting), the subgroup of *Cmcm*. Interestingly, *Cmcm* is the space group expected above 600 K at ambient pressure or above a pressure of 6 GPa at ambient temperature [19]. It is important to notice that in *Cmcm*, the two ladders of the unit cell are parallel and equivalent by translation. It is not the case in the *Pnma* structure. Most importantly, both space groups are polar, contrary to the *Pnma*, which indicates that $BaFe_2Se_3$ is ferroelectric already at room temperature.

We have refined the 300 K data obtained for the samples *S*1 and *S*2 in both space groups. What one immediately sees is that the refinement in the *Pmmn* space group leads to poor reliability factors ($R_{obs} \approx 30$) while the refinement in $Pmn2_1$ was of high quality ($R_{obs} \approx 3$). Table I presents the atomic parameters of the 300 K structure of the sample *S*1. For the sample *S*2, the refined structure is equivalent within the error bars given in Table I.

From the refined structure in the $Pmn2_1$ space group, one observes that the dimerization of the chains forming the ladders is much stronger than for the structures previously published. The difference of Fe-Fe distances along the dimerized chains reaches 0.13 ± 0.05 Å in our refinement while it is ten times smaller (0.007 and 0.014 Å, respectively) in the structures of [20] and [9]. However, a recent neutron experiment using a PDF analysis also evidenced a strong Fe-Fe dimerization of about 0.2 Å [6].

Concerning the ladder, we show here that there is no more symmetry element relating its two chains as the inversion center is suppressed. It is, however, interesting to notice that within the error bars, two facing stiles of one ladder are nearly identical. This pseudosymmetry corresponds to a mirror **m** as present in the space group *Pmmn*. However, the *Pmmn* symmetry also imposes the two ladders of the unit cell to be parallel. This is obviously not the case as the optimal refinement gives a relative tilt between ladders of nearly 6°. This is corroborated by the fact that the refinement using the *Pmmn* space group is of poor quality.

TABLE I. Atomic positions of $BaFe_2Se_3$ at 300 K in the $Pmn2_1$ space group ($R_{obs} = 3.29\%$, $wR_{obs} = 6.41\%$). The lattice parameters are $a = 5.4437(3)$ Å, $b = 11.8710(5)$ Å, and $c = 9.1629(4)$ Å, $\alpha = \beta = \gamma = 90°$. The number of reflections which $I > 3_\sigma$ is 2471.

Atom	Site	x	y	z
Ba1_1	2*a*	0.5	0.43618(19)	−0.5209(3)
Ba1_2	2*a*	0	0.06672(18)	0.5181(3)
Fe1_1	4*b*	0.2442(4)	0.7446(3)	−0.3496(7)
Fe1_2	4*b*	0.2438(4)	−0.2436(3)	0.3528(7)
Se1_1	2*a*	0.5	0.6111(3)	−0.2271(6)
Se1_2	2*a*	0	−0.1061(3)	0.2291(6)
Se2_1	2*a*	0.5	0.8716(3)	−0.4902(6)
Se2_2	2*a*	0	−0.3806(3)	0.4925(6)
Se3_1	2*a*	0.5	0.6515(3)	−0.8135(5)
Se3_2	2*a*	0	−0.1457(3)	0.8149(5)

Following our result, one finds that the two ladders of the unit cell are symmetry equivalent by the **n** glide plane and the 2_1 screw axis. Consequently, there are four different Fe-Fe distances (2.785, 2.659, 2.789, and 2.655 Å) in the structure to be compared to the two very close Fe-Fe distances (2.72 ± 0.01 Å) observed in the previous structures [9,20].

Let us now consider the 150 K structure which describes the structure of $BaFe_2Se_3$ below the Néel transition and thus in the $k = (0.5\ 0.5\ 0.5)$ magnetic phase. The apparition of reflections breaking the **n** glide plane implies that the $Pmn2_1$ space group is no more acceptable. The low-temperature structure seems to be affected by the magnetic ordering. The magnetic transition being second order, we expect a structure subgroup of $Pmn2_1$. The unique space group compatible with all the experimentally observed reflections is $Pm11$ ($P1m1$ in the standard setting, labeled *Pm* in the following). *Pm* is monoclinic with unit cell parameters close to orthorhombic ones ($\beta \approx 90.05 \pm 0.05°$). It is interesting to see that the possible magnetic subgroups of $Pmn2_1$ with the magnetic propagation wave vector k are monoclinic, thus perfectly compatible with our result. We have refined the 150 K data and obtained the structure given in Table I of the Supplemental Material. As expected we observe eight different Fe-Fe distances because the ladders are no more equivalent by symmetry. The dimerization now strongly differs between the two ladders of the unit cell (a mean dimerization of 0.25 ± 0.03 Å for one ladder and 0.07 Å for the other).

To better use the $Pmn2_1$ and *Pm* experimental structures we roughly evaluated the associated polarization using a simple ionic summation of Ba^{2+}, Fe^{2+}, and Se^{2-} ions. Of course a correct calculation should be done using a Berry phase approach within a DFT calculation; however, such an easy procedure provides an order of magnitude. For the $Pmn2_1$ group we used as reference the closest *Pnma*

non polar structure and for the *Pm* group we used the closest $P2_1/m$ non polar structure. Under these conditions we found a polarization of 0.8 mC/m^2 along the c direction for the $Pmn2_1$ structure, as expected from symmetry considerations. This value is comparable to the electric polarization of improper multiferroics such as RMn_2O_5 [21]. It is also very close to the polarization's amplitude proposed after density functional theory (DFT) calculations in the magnetic phase by [2]. However, in this work, the authors predict the electric polarization to be due to an exchange-striction effect. We show here that the electric polarization is already present at ambient temperature in the paramagnetic phase and cannot be ascribed to a magnetoelectric mechanism.

The same calculation of the ionic polarization performed in the magnetic phase at 150 K corresponding to the *Pm* structure gives a much larger value 4 mC/m^2. The symmetry imposes the polarization to be in the (a, c) plane (in the *Pm* setting), which means perpendicular to the ladder direction and mainly along the rung direction (**a**) ($p_a = 3.6$ mC/m^2 and $p_c = 1.8$ mC/m^2). We have tried to experimentally measure the hysteresis cycle associated with the electric polarization at 300 and 150 K. However, the system is only weakly localized, the electronic gap has been measured to be about 250 meV, and the longitudinal resistivity remains quite low, around 10 Ω cm at 300 K. We therefore encountered electronic charge leakage even at low temperature. This prevented from the detection of the ionic polarization. Such an effect is well known in organic conductors such as $TMTTF_2X$. Importantly, recent preliminary second harmonic generation measurements, confirmed the absence of inversion center [22].

In conclusion, our work rules out the room temperature structure of $BaFe_2Se_3$ as known until now. The structure we propose is polar with an electric polarization along the rung of the Fe ladders. In the magnetic phase, the structure is modified and the electric polarization is strongly enhanced as well as tilted with respect to the rung direction. The system becomes multiferroic with a high Néel temperature and a strong electric polarization. $BaFe_2Se_3$ thus presents an ideal multiferroic behavior. As for the superconducting state which is in competition with the multiferroic ground state under pressure, its stabilization remains an issue of tremendous importance. The presence of eight different Fe-Fe distances in the *Pm* structure at low temperature has now to be considered in the theoretical models involving the $(t$-$J)$ competition [23].

We would like to acknowledge P. Fertey and S. Rouzière for fruitful discussions. We thank F. Damay and the Laboratoire Léon Brillouin (France) for the neutron diffraction experiment used to determine T_N. This work was supported by the Chinese Scholarship Council project (No. 201806830111).

[1] J. M. Caron, J. R. Neilson, D. C. Miller, A. Llobet, and T. M. McQueen, Phys. Rev. B **84**, 180409(R) (2011).
[2] S. Dong, J. M. Liu, and E. Dagotto, Phys. Rev. Lett. **113**, 187204 (2014).
[3] J. Ying, H. Lei, C. Petrovic, Y. Xiao, and V. V. Struzhkin, Phys. Rev. B **95**, 241109(R) (2017).
[4] A. Georges, L. de Medici, and J. Mravlje, Annu. Rev. Condens. Matter Phys. **4**, 137 (2013).
[5] J. Rincón, A. Moreo, G. Alvarez, and E. Dagotto, Phys. Rev. Lett. **112**, 106405 (2014).
[6] J. M. Caron, J. R. Neilson, D. C. Miller, K. Arpino, A. Llobet, and T. M. McQueen, Phys. Rev. B **85**, 180405(R) (2012).
[7] S. W. Lovesey, D. D. Khalyavin, and G. van der Laan, Phys. Scr. **91**, 015803 (2016).
[8] J. Herbrych, N. Kaushal, A. Nocera, G. Alvarez, A. Moreo, and E. Dagotto, Nat. Commun. **9**, 3736 (2018).
[9] Y. Nambu, K. Ohgushi, S. Suzuki, F. Du, M. Avdeev, Y. Uwatoko, K. Munakata, H. Fukazawa, S. Chi, Y. Ueda, and T. J. Sato, Phys. Rev. B **85**, 064413 (2012).
[10] H. Lei, H. Ryu, A. I. Frenkel, and C. Petrovic, Phys. Rev. B **84**, 214511 (2011).
[11] See Supplemental Material at http://link.aps.org/supplemental/10.1103/PhysRevB.101.020101 for the characterization details of the samples, the susceptibility measurements, the neutron diffraction results and more refinement details at 150 K.
[12] M. Mourigal, S. Wu, M. B. Stone, J. R. Neilson, J. M. Caron, T. M. Mcqueen, and C. L. Broholm, Phys. Rev. Lett. **115**, 047401 (2015).
[13] X. Liu, C. Ma, C. Hou, Q. Chen, R. Sinclair, H. Zhou, Y. Yin, and X. Li, Europhys. Lett. **126**, 27005 (2019).
[14] J. Gao, Y. Teng, W. Liu, S. Chen, W. Tong, M. Li, X. Zhao, and X. Liu, RSC Adv. **7**, 30433 (2017).
[15] B. Saparov, S. Calder, B. Sipos, H. Cao, S. Chi, D. J. Singh, A. D. Christianson, M. D. Lumsden, and A. S. Sefat, Phys. Rev. B **84**, 245132 (2011).
[16] W. J. Schutte and J. L. De Boer, Acta Crystallogr. **B44**, 486 (1988).
[17] K. Hirota, D. E. Cox, J. E. Lorenzo, G. Shirane, J. M. Tranquada, M. Hase, K. Uchinokura, H. Kojima, Y. Shibuya, and I. Tanaka, Phys. Rev. Lett. **73**, 736 (1994).
[18] V. Petříček, M. Dušek, and L. Palatinus, Z. Kristallogr. **229**, 345 (2014).
[19] V. Svitlyk, D. Chernyshov, E. Pomjakushina, A. Krzton-Maziopa, K. Conder, V. Pomjakushin, R. Pottgen, and V. Dmitriev, J. Phys.: Condens. Matter **25**, 315403 (2013).
[20] H. Hong and H. Steinfink, J. Solid State Chem. **5**, 93 (1972).
[21] V. Balédent, S. Chattopadhyay, P. Fertey, M. B. Lepetit, M. Greenblatt, B. Wanklyn, F. O. Saouma, J. I. Jang, and P. Foury-Leylekian, Phys. Rev. Lett. **114**, 117601 (2015).
[22] T. Aoyama, S. Imaizumi, T. Togashi, Y. Sato, K. Hashizume, Y. Nambu, Y. Hirata, M. Matsubara, and K. Ohgushi, Phys. Rev. B **99**, 241109(R) (2019).
[23] W. Lv, A. Moreo, and E. Dagotto, Phys. Rev. B **88**, 094508 (2013).